

Studies on Liquid Flow through the Model of the Crystallizer Segment

Witold Suhecki, Marian Trafczynski*

Institute of Mechanical Engineering, Faculty of Civil Engineering, Mechanics and Petrochemistry, Warsaw University of Technology, Lukasiewiczza 17, 09-400 Plock, Poland
 Marian.Trafczynski@pw.edu.pl

In the sugar industry, in the process of crystallizing the suspension of the afterproduct (crystals III), among others cooling crystallizers with vertically moving tubular cooling elements are utilized. According to the designers and users, in this crystallizer type there is potential for heat transfer intensification leading to a significant reduction of the apparatus dimensions. Liquid flow through the model of a single tubular segment (part of the moving cooling element) of the cooling crystallizer was studied. An experimental model of the crystallizer segment was built. The model was utilized for the experimental research on liquid flow, conducted in parallel with the simulation of the segment operation. The method of digital particle image velocimetry was applied to analyze the experimental flow. The experimental results enabled verification of the assumptions of the numerical model based on CFD code Fluent. The finite volume method was applied in the numerical simulation. The results of experimental research and of numerical simulations were presented to improve understanding of physical conditions that promote or disturb homogenous velocity distribution of the liquid flowing around the segment of the crystallizer model.

1. Introduction

The paper presents a study on liquid flow through the model of a single segment of the cooling crystallizer with vertically moving cooling elements. Parameters of an industrial crystallizer for crystal slurry III, operated in a Polish sugar factory were considered when building the experimental model (Suhecki, 2008). According to the designers and users of this type of crystallizers, there are potential opportunities for heat transfer intensification which is a proven technique to make significant reduction in the dimensions of heat-exchange equipment possible (Kapustenko et al., 2015).

From the scientific point of view, the problem to be considered is the laminar flow of a liquid through the system of cooling tubes arranged in parallel, which in engineering practice is considered as a single object - a tube bundle.

Experimental studies of turbulent flow around a tube bundle at Reynolds numbers in the range from 5,400 to 29,700 were presented by Iwaki et al. (2004).

Simulation studies of the effect of changing the distance between the tubes in the transverse tube bundle on the homogeneity of the flow field behind a row of tubes, for Reynolds number 150, were conducted by Huang et al. (2006). They demonstrated a significant impact of tube distance from the wall on the formation and size of the vortex path behind the row of tubes.

The aim of the present study was to examine what physical conditions are conducive to, and which ones interfere with, the formation of a uniform flow-velocity distribution of the liquid flowing through the model of a tube bundle at Reynolds number below 1. Experimental studies and numerical simulation of the operation of the crystallizer segment were carried out. To the knowledge of the present authors, no studies of liquid flow induced by the movement of a tube bundle for Reynolds numbers less than 1 have so far been reported in the literature.

2. Materials and methods

Experimental tests were carried out using the method of Particle Image Velocimetry (PIV); its applications in the studies on process equipment design were presented by Suchecki (2014) and Ge et al. (2014). The results of PIV-based measurements allowed verifying the assumptions of the numerical simulation model based on CFD code Fluent.

The experiments were performed on a moving model of the tube bundle (crystallizer segment) immersed in a liquid. The focus was on flow-velocity fields in the liquid surrounding the tube bundle. The CCD camera was placed in front of the tube bundle and remained stationary with respect to it (moved together with the model). In the following, liquid flow around the tube bundle will be discussed; actually though, the bundle was moving relative to the liquid.

The tube bundle model was designed and built maintaining hydrodynamic and geometrical similarity with the real crystallizer segment. The geometric scale was 1:20.

2.1 Experimental set-up for Particle Image Velocimetry (PIV) experiments

A view of the test stand is shown in Figure 1.

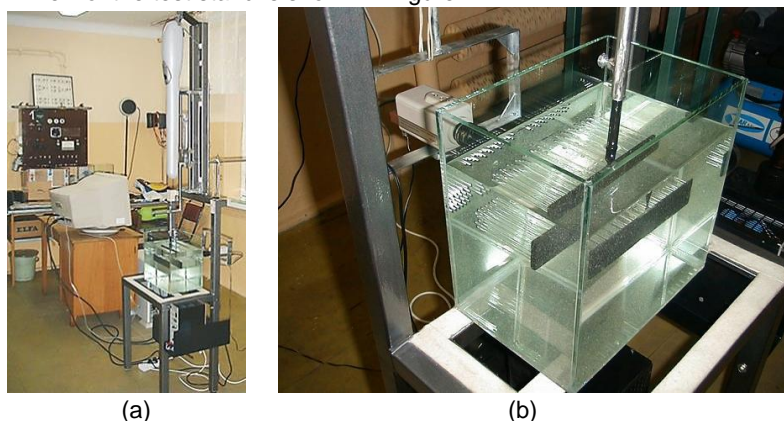


Figure 1: General view of the test stand (a). View of the tube bundle model and camera (b)

The tube bundle model illuminated by a light sheet perpendicular to the optical axis of the camera is shown in Figure 2.

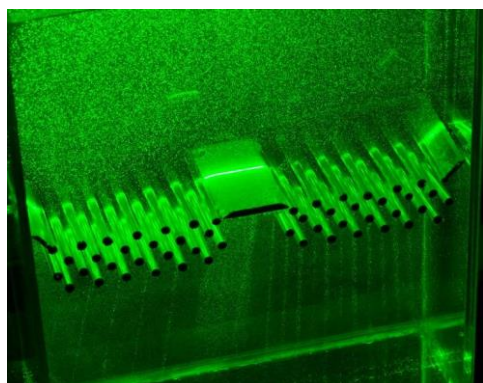


Figure 2: Tube bundle model illuminated by laser-light sheet

Experiments were conducted at tube-bundle velocity in the range from $1.7 \cdot 10^{-3}$ to $12.9 \cdot 10^{-3}$ m/s and two camera angles (normal – to cover the whole model and zooming – to show parts of the model). The liquid used in the experiments was water-glycerol mixture with glycerol concentration 90 %, density $1,235 \text{ kg/m}^3$ and kinematic viscosity $187 \cdot 10^{-6} \text{ m}^2/\text{s}$. A summary of experimental conditions including the values of model velocity and Reynolds number (calculated with respect to the diameter of a single tube) of the liquid flow through the tube bundle is given in Table 1. The Reynolds number is defined as:

$$Re = \frac{Vd}{\eta} \quad (1)$$

where: V – velocity of the tube bundle [m/s], d – tube diameter [m], η – kinematic viscosity of liquid [m²/s]. The measurement system consisted of the laser dual-Nd:YAG, New Wave 120XT-15Hz and high-speed pco.1200hs camera. The velocity field in the liquid surrounding the tube bundle was determined on the basis of recorded flow images using PIV anemometry (Suchecky, 2014).

Table 1: Summary of the flow velocity and Reynolds number of the liquid flow relative to the tube bundle

	Flow velocities	Reynolds number		Flow velocities	Reynolds number
	[m/s]	[-]		[m/s]	[-]
Move up	$1.7 \cdot 10^{-3}$	$9.5 \cdot 10^{-3}$	Move down	$2.2 \cdot 10^{-3}$	$12.5 \cdot 10^{-3}$
	$4.3 \cdot 10^{-3}$	$24.5 \cdot 10^{-3}$		$4.8 \cdot 10^{-3}$	$27.4 \cdot 10^{-3}$
	$7.0 \cdot 10^{-3}$	$39.4 \cdot 10^{-3}$		$7.5 \cdot 10^{-3}$	$42.2 \cdot 10^{-3}$
	$9.7 \cdot 10^{-3}$	$54.7 \cdot 10^{-3}$		$10.1 \cdot 10^{-3}$	$57.3 \cdot 10^{-3}$
	$12.2 \cdot 10^{-3}$	$68.9 \cdot 10^{-3}$		$12.9 \cdot 10^{-3}$	$72.9 \cdot 10^{-3}$

2.2 CFD simulations

The finite volume method was applied to numerically simulate liquid flow in the model of the crystallizer segment. Computer simulations were carried out using commercial CFD software Fluent (versions 5.5 and 6.1) of FLUENT Inc. Another software product of the same company, GAMBIT (versions 1.3 and 2.0) was applied as a preprocessor. Detailed computational models used for the simulation of liquid flow in the experimental model were selected so as to maintain dynamic similarity to the industrial cooling crystallizer. Since the experimental studies resulted in determining velocity fields in the planar slices of the liquid illuminated by laser-light sheets, two-dimensional modelling was adopted for the numerical simulations. Additionally, numerical experiments to study the effect of design changes on the characteristics of liquid flow in the crystallizer were carried out. The studies included the effect of the distance between the guide vanes and the vessel wall, of the distance between the pipes and of the application of extra vanes at the bottom of the tube bundle, on the velocity fields in the liquid. Non-structural grids of triangular elements were used in all the numerical models. Geometrical models together with superimposed grids are visualized in Figure 3. The model shown in Figure 3a is a representation of the basic geometry of the crystallizer segment and at the same time, of the experimental reference model. In the model shown in Figure 3b, the guide vanes are moved away from the vessel wall by a distance equal to the tube diameter. The guide vanes and the baffle were removed from the model shown in Figure 3c and tube spacing was increased in such a way that the distance between the wall and the bundle was equal to the tube diameter and the width of the channel in the vessel centre was equal to twice the tube diameter. The number of tubes and the distance between the tube rows remained unchanged, also in the model shown in Figure 3d in which both guide vanes and baffles placed above and below the tube bundle were employed.

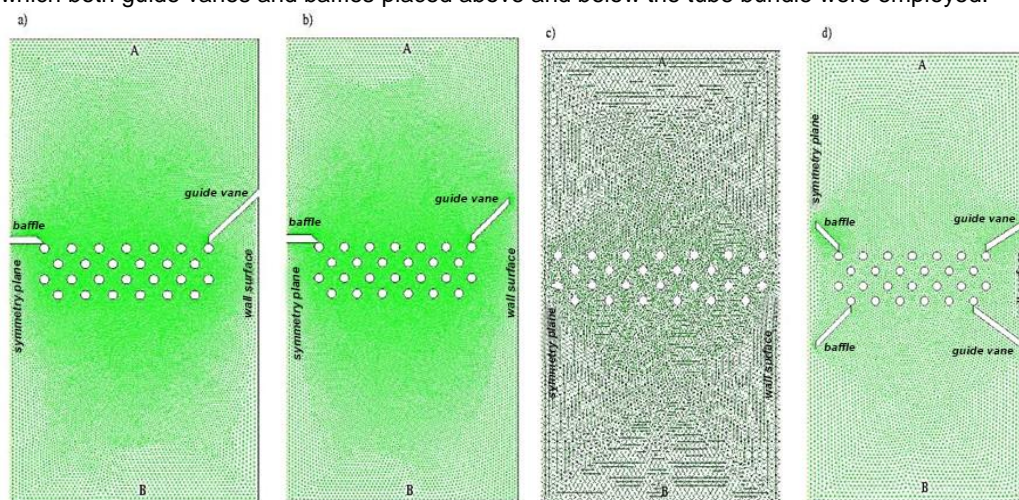


Figure 3: Computational grids used in the simulations. The number of grid elements: a) 51 142 b) 54 180, c) 17 620, d) 21 576

3. Results and discussion

Examples of velocity field distribution of the liquid flow around the tube bundle are shown in Figures 4-6. Flow-velocity maps are accompanied by the legends containing explanation of velocity values determined by the least-squares method.

The areas below the lower row of tubes and above the upper one were studied to check the uniformity of velocity fields below and above the tube bundle by determining velocity profiles within four tube diameters above. In the charts, these locations are indicated by horizontal lines, and the corresponding velocity profiles are placed above and below the graph. This made it possible to determine how the velocity of the tube bundle affected the uniformity of the liquid-velocity fields remote from the tube bundle.

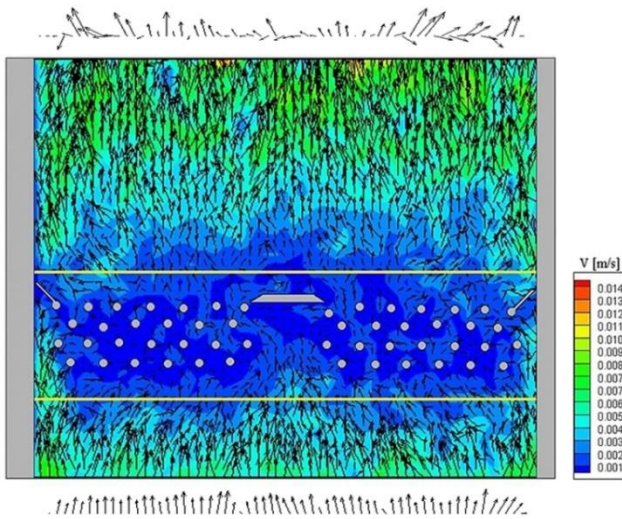


Figure 4: Velocity field distribution in the liquid for downward movement of the tube bundle (standard camera view). Velocity of the tube bundle $2.2 \cdot 10^{-3}$ m/s, $Re = 12.5 \cdot 10^{-3}$

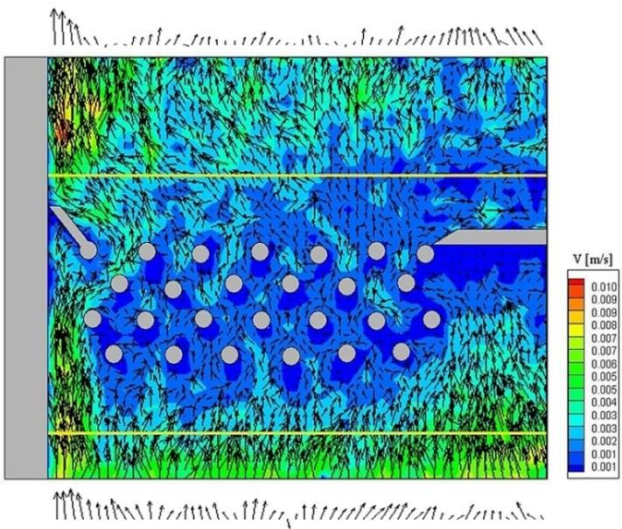


Figure 5: Velocity field distribution in the liquid for downward movement of the tube bundle (zooming view). Velocity of the tube bundle $2.2 \cdot 10^{-3}$ m/s, $Re = 12.5 \cdot 10^{-3}$

The values of liquid-flow velocity in the regions between the tubes are very small while those of the liquid flowing along vessel walls and in the middle of the model are significantly higher due to lower hydraulic resistance of these regions (Figure 4 and 5). Zooming views recorded during the downward movement of the model reveal that there was no movement of the liquid in the regions close to the baffle and guide vanes. "Dead" areas were forming beneath these which implies that the liquid flow along the wall is influenced by the guide vanes and

directed to the space between the tubes. However, the “pushed” fluid flows around only a small part of the tube bundle, as can be seen in Figure 6. Increased velocity of the bundle does not influence the formation of “dead” areas. It was also found that the velocity profiles below the tube bundle are more uniform than the velocity profiles above the bundle.

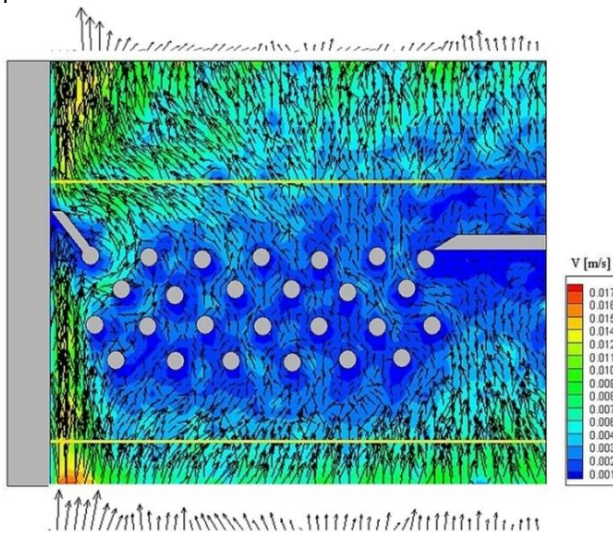


Figure 6: Velocity field distribution in the liquid for downward movement of the tube bundle (zooming view). Velocity of the tube bundle $12.9 \cdot 10^{-3}$ m/s, $Re = 72.9 \cdot 10^{-3}$

The distribution of local flowrates was also analysed considering three parts of the model: close to the vessel wall, between the tubes and the central part. The obtained results indicate that the higher the velocity of the tube bundle, the lower is the share of flowrate in the area between the tubes – both at upward and downward movement of the tube bundle.

Adopting the approach frequently applied in process engineering studies (exemplified by Cuervo et al., 2014), the experimental results were used to verify the assumptions of the numerical reference model based on the CFD code Fluent. A high degree of similarity between the experimental results and the results of numerical simulations (Figure 7) enabled carrying out simulations also for other models (geometrically different from the reference model) shown in Figure 3.

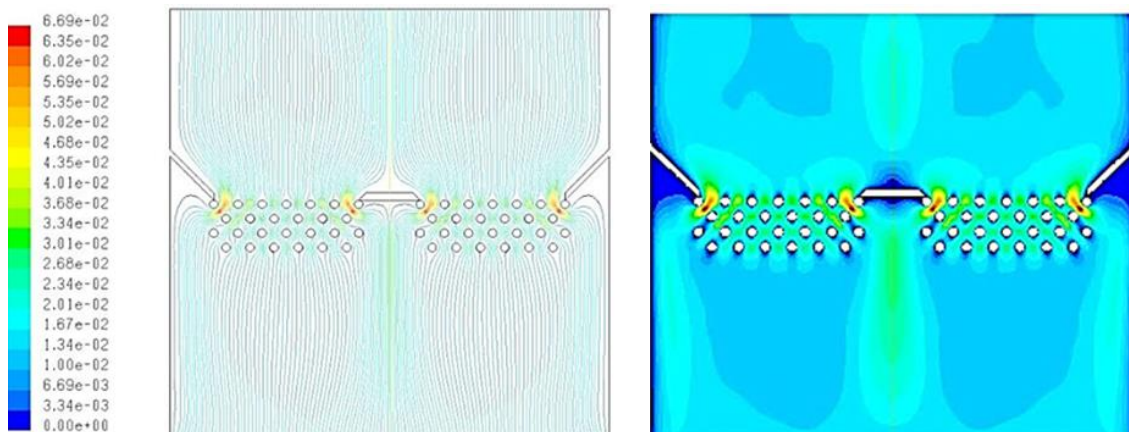


Figure 7: Streamlines (left) and distribution of the flow-velocity field (right) during the liquid flow around the tube bundle. Bundle velocity $2.2 \cdot 10^{-3}$ m/s, $Re = 12.5 \cdot 10^{-3}$

The computations were performed for the values of liquid flow velocity shown in Table 1. The analysis of simulation results proved that changes in the velocity of the tube bundle have a negligible effect on the flow velocity profiles above and below the bundle. More profound are the effects of changes in the geometry of the tube bundle. Figure 8 shows two flow-velocity fields around the tubes determined for two geometrically different tube bundles.

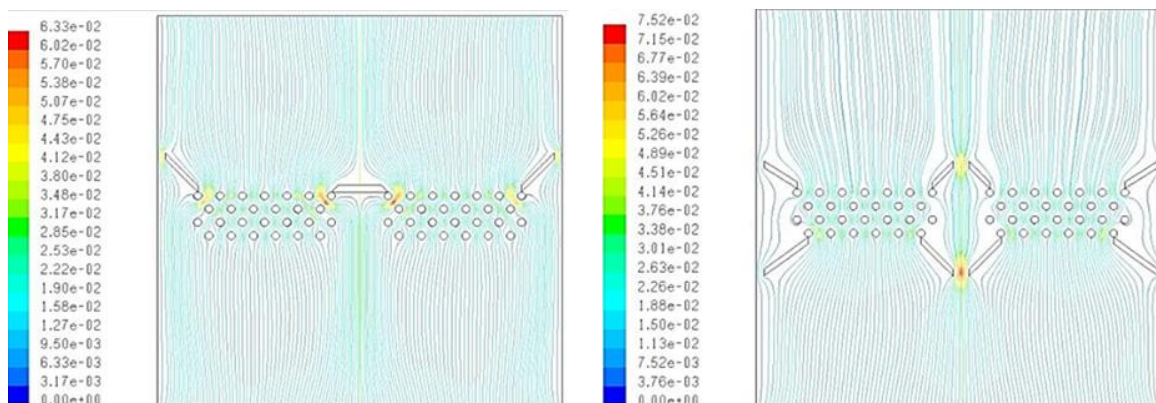


Figure 8: Visualisation of the distribution of flow-velocity field: tube bundle equipped with a baffle in the center and two guide vanes at the vessel wall (left), and tube bundle with four baffles and four guide vanes (right)

4. Conclusions

The obtained research results indicate that for given design parameters of the crystallizer, numerical simulation makes it possible to evaluate the quality of flow-velocity distribution of the liquid flowing around the cooling tubes. Information obtained on the basis of experimental and simulation studies on the liquid flow around the specific moving tube bundle can be summarized as follows. In the studied range of tube-bundle velocity, laminar flow was established in the areas between the tubes. A large percentage of the total flowrate passed through the central part of the model and its part close to vessel walls where the local hydraulic resistances are lower than that of the main part of the tube bundle. By applying a baffle and guide vanes, for the downward and upward movement of the model an average increase of about 15% in the percentage of liquid flowrate through the main part of the tube bundle was obtained, compared with the reference model. There was no movement of the liquid in the areas just below the baffle and guide vanes. Owing to the influence of the baffle and guide vanes, the liquid flowrate through the main part of the tube bundle is further increased by 5 % during upward movement of the model. The most favourable distribution of local flowrates through the different parts of the model is obtained at $Re = 9.5 \cdot 10^{-3}$, that is, at model velocity of $1.7 \cdot 10^{-3}$ m/s.

The percentage of the flowrate passing between the tubes is gradually decreased with the increase in model velocity for both upward and downward movements; simultaneously, the percentage of local flowrates along the wall and in the central part of the model is increased. Increased tube spacing reduces the local hydraulic resistance of the tube bundle and leads to the liquid flow more uniformly distributed over the cross-section of the apparatus.

References

- Cuervo N., Murillo C., Dufaud O., Bardin-Monnier N., Skali-Lami S., Remy J.F., Auzolle P., Perrin L., 2014, Combining CFD simulations and PIV measurements to optimize the conditions for dust explosion tests, *Chemical Engineering Transactions*, 36, 259-264, DOI: 10.3303/CET1436044.
- Ge H-W., Norconk M., Lee S-Y., Naber J., Wooldridge S., Yi J., 2014, PIV measurement and numerical simulation of fan-driven flow in a constant volume combustion vessel, *Applied Thermal Engineering*, 64, 19-31, DOI: 10.1016/j.applthermaleng.2013.11.073.
- Huang Z., Olson J.A., Kerekes R.J., Green S.I., 2006, Numerical simulation of the flow around rows of cylinders, *Computers & Fluids*, 35, 485-491, DOI: 10.1016/j.compfluid.2005.03.001.
- Iwaki C., Cheong K.H., Monji H., Matsui G., 2004, PIV measurement of the vertical cross-flow structure over tube bundles, *Exp. in Fluids*, 37(6), 350-363, DOI: 10.1007/s00348-004-0823-1.
- Kapustenko P.O., Kukulka D.J., Arsenyeva O.P., 2015, Intensification of heat transfer processes, *Chemical Engineering Transactions*, 45, 1729-1734, DOI: 10.3303/CET1545289.
- Sucheckı W., 2014, Research on liquid flow in industrial apparatuses by means of both visualization and numerical simulation methods, WUT Publishing House, Warsaw, Poland (in Polish).
- Sucheckı W., 2008, Study of suspension flow by crystallizer segment model, In collective work: Selected problems of liquid flow and heat transfer, ed. W. Sucecki, 23-57, WUT Publishing House, Warsaw, Poland (in Polish)